Surface Nature of UV Deterioration in Properties of Solid Poly(ethylene terephthalate)

WEI WANG, ATSUSHI TANIGUCHI, MOTOTADA FUKUHARA, TAKEHIKO OKADA

Synthetic Fibers Laboratory, Fibers and Textiles Research Laboratories, Toray Industries, Inc., Mishima 4845, Shizuoka 411, Japan

Received 11 September 1996; accepted 31 May 1997

ABSTRACT: We investigated the changes in the molecular weight and also in the mechanical properties with the distance to the exposed surface of the irradiated stacked poly(ethylene terephthalate) (PET) film samples. A relation between the molecular weight and the mechanical properties of the irradiated PET was established. The relation demonstrates that the decrease in molecular weight is one of the main origins causing the deterioration in the mechanical properties. The photodegradation process developing in PET was quantitatively studied by investigating the degradation kinetics of stacked PET film samples. Our results show that the strongest degradation takes place at the exposed surface, and the degradation rate decreases with increasing the distance. This further implies that the capability to bear a tensile stress in the area near the exposed surface is much lower than that in bulk. Therefore, irradiated PET may be fractured in a lower stress. These results indicate the surface nature of ultraviolet deterioration in the physical properties of PET. © 1998 John Wiley & Sons, Inc. J Appl Polym Sci **67:** 705–714, 1998

Key words: poly(ethylene terephthalate); UV deterioration; molecular weight; mechanical properties; surface nature

INTRODUCTION

The ultraviolet (UV) light deterioration in the properties of polymers has been studied extensively. The important literature coverage on photodegradation, photooxidation, and photostabilization of polymers can be found in Ranby and Rabek[1] and Rabek.[2] Many studies on this subject were motivated by the large number of outdoor applications for polymers as films, bulk or molded forms, and fibers, and also by the great effect of UV radiation on their mechanical and other properties. Many studies for aromatic polyesters and other polymers have indicated the deterioration in the mechanical properties of polymers stemming primarily from the photodegradation of macromolecules after irradiation.[1–7]

Most of the early experimental studies on photodegradation kinetics of polymers were mainly conducted within their dilute solution by determining the change in molecular weight caused by irradiation.[8–11] The results are very consistent with those predicted by some theories for photodegradation kinetics of polymers based on the assumption that all macromolecules in a system have the same probability of their undergoing degradation caused by UV radiation.[8,11] It is, however, important to understand how the photodegradation process develops in solid polymers and to determine how the degradation in molecular weight affects the properties, in particular, mechanical properties, of solid polymers. Some studies have dealt theoretically[12–13] and experimentally[14–20] with these issues by using film samples. The results obtained from aromatic polyesters

Correspondence to: T. Okada.

Journal of Applied Polymer Science, Vol. 67, 705–714 (1998)
 CCC 0021-8995/98/040705-10

have shown the surface nature of the UV degradation and the strongest degradation occurring in the area near the exposed surface.[14–20] Unfortunately, these published results are not enough for indicating how the photodegradation process develops in solid polymers and, further, how it influences the properties of polymers because most of the experiments were conducted with a single polymer film.

The work described in this article is connected with the investigations of the photodegradation kinetics of poly(ethylene terephthalate) (PET) film and of the influence of UV irradiation on its mechanical properties. The radiation experiment was conducted with stacked PET film samples. The intrinsic viscosity of each layer was measured after irradiated; and, hence, the relation between the number-average molecular weight and the distance to the exposed surface was obtained. Correspondingly, the mechanical properties of each layer were measured, and the relation between the mechanical properties and the distance was also obtained. On the basis of these data, the relationship between molecular weights and mechanical properties of the PET samples was established; and, further, the photodegradation kinetics occurring in each PET layer of the stacked samples were studied. These results indicate that the photodegradation process developing in the PET sample is of a surface nature; namely, the strongest photodegradation takes place at the exposed surface of the sample. The important origin, which results in a rapid deterioration of mechanical properties of irradiated PET products, is discussed in this article.

EXPERIMENTAL

Materials

The PET film used is a commercial film (TORAY "LUMIRROR 4YC21") with a thickness of 4.4 μm and a density of 1.397 g/cm^{-3}. A few pieces of films with a size of 200 $\times$ 150 mm were arranged in stack, then this stacked film sample was bound on the surface of a flexible paperboard with a thickness of 0.5 mm and through which light penetrates.

Irradiation

Figure 1 schematically shows the irradiator used in this work. It consists of six fluorescent sunlamps, a cylindrical sample support, and a metal drum coated in white. The diameters and lengths of the drum and the sample support are ϕ430 and 700 mm, and ϕ100 and 350 mm, respectively. Six fluorescent sunlamps (Toshiba FL20S-E) are equally distributed in the drum. The sunlamp has a spectral distribution of the radiation energy at 280–400 nm and a single maximum of the radiation energy at about 313 nm. Since PET is sensitive to the light at about 314 nm,[15] an accelerated testing of PET photodegradation was conducted in this work. The length of the lamp is 595 mm longer than the length of the sample. The stacked samples bound on the paperboard were fixed on the sample support, which rotated concentrically during irradiation. Therefore, the light was well distributed on the sample surface. The sample-to-lamp distance used was 100 mm. Irradiation was carried out at an operating temperature of 48–56°C, which is lower than the glass transition temperature of PET, with no control of the relative humidity. Only one surface of the stacked film samples was irradiated in this work since the paperboard was used.

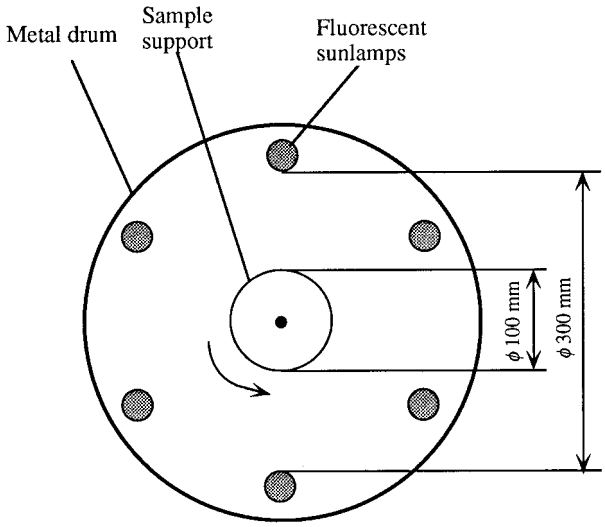

Figure 1 Schematic representation of the irradiator used in this work. It consists of six fluorescent sunlamps, a cylindrical sample support, and a metal drum coated into white.

Viscosity Measurements

Solution viscosities of the PET samples before and after irradiation were measured at 25°C in *o*-chlorophenol in an Ostward viscometer. The intrinsic viscosities [η] of solutions were determined by ex-

trapolation of η_{sp}/c versus c plot to zero concentration. Number-average molecular weights were related to intrinsic viscosities by[21]

$$[\eta] = 3.0 \times 10^{-4} \times \bar{M}_n^{0.77}. \quad (1)$$

Measurements of Mechanical Properties

For determining the mechanical properties of PET film samples before and after irradiation, the original film was cut into the 160 × 10 mm strips by using a razor. The strips as the first layer were directly irradiated; but the strips following the first were covered by the same PET films, of which the size was larger than the strip, and then were irradiated. The load and elongation values of original and irradiated strips were measured by using a Tensilon device (UCT-100) at 25°C. The separation of the crossheads was 100 mm, and the separating speed of the crossheads was 500 mm/min^{-1}. In this work, five strip specimens were used for the measurement, and the average value was obtained after deleting the highest and lowest points.

RESULTS AND DISCUSSION

Before we present the experimental results, we indicate below that two factors, the light reflections at film–air interfaces in the stacked film sample and the fluctuation of the operating temperature used during irradiation, may affect the experimental results more or less. The reflections are approximately 5% at each interface, as pointed out in Schultz and Leahy.[15] In this work, the operating temperature changed in the range of 48–56°C but it was lower than the glass transition temperature of PET (~ 69°C for amorphous PET). Therefore, this fluctuation will not strongly affect the photodegradation of PET, as pointed out in Dan and Guillet.[17] Since the two factors have no great influence, in this study, we neglect them for the sake of convenience. However, neglecting the light reflection will lead to an underestimation of UV deterioration in the physical properties developed inside PET.

Change in Molecular Weight

Figure 2 shows a plot of the number-average molecular weight $\bar{M}_n$ against the distance x to the exposed surface for the stacked film samples irradiated for 10, 30, and 50 h. Since the PET film has the thickness of 4.4 μm, each point in Figure 2 shows the average value of $\bar{M}_n$ obtained from the film. This feature is shown by a 4.4 μm bar in Figure 2. The figure shows that the value of $\bar{M}_n$ depends on the position of the layer in the stacked film samples. $\bar{M}_n$ determined from the first layer is the smallest one and then it increases with x. This simply implies that the strongest degradation of the macromolecules takes place in the first layer of the stacked film samples.

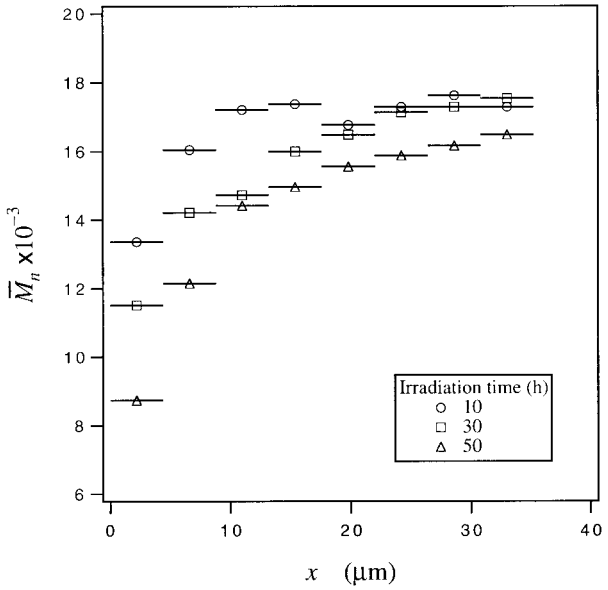

Figure 2 Plot of the number-average molecular weight $\bar{M}_n$ obtained from the irradiated film samples in stack against the distance to the exposed surface x. The irradiation times are indicated in the figure.

Change in Mechanical Properties

Figure 3 shows some typical load–elongation curves of the irradiated strips at the first layer after irradiated for different times. The irradiation times are 0, 2, 5, 10, 20, 30, 40 h, respectively, as indicated in the figure. All curves show that the irradiated samples yielded at the same stress ($\sigma^y \approx 120$ MPa) and strain ($\varepsilon^y \approx 4\%$) but broke at the different stresses and strains. The stress (σ^*) and strain (ε^*) at break decrease with the irradiation time t. For the original strip, $\sigma_0^* \approx 265$ MPa and $\varepsilon_0^* \approx 115\%$ at break. The margin of errors induced in preparation of the PET strips and during measurement is estimated at about 5% for σ^* and 10% for ε^*, respectively. Figure 3 shows that σ^* and ε^* decrease with t. At $t = 30$

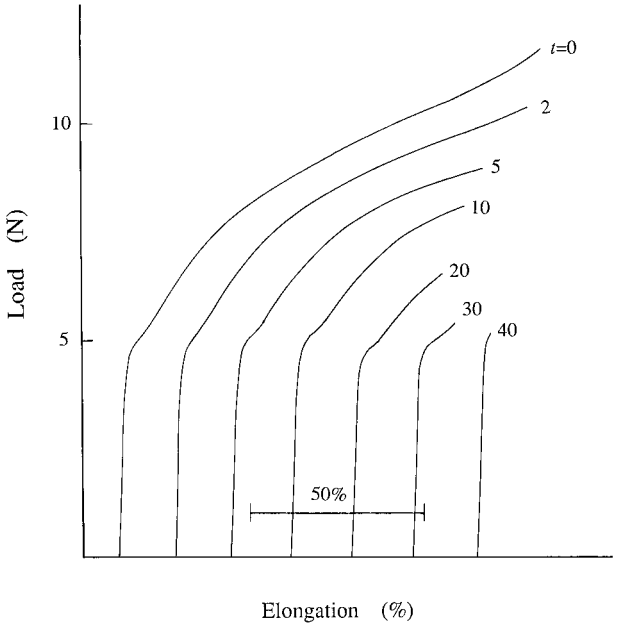

Figure 3 Load–elongation curves of irradiated PET strips at the first layer. The irradiation times are indicated in the figure.

h, σ^* and ε^* of this sample are very close to its σ^y and ε^y. At $t = 40$ h, the irradiated strip broke immediately after yielded at $\sigma^y \approx 120$ MPa and $\varepsilon^y \approx 4\%$; thus, $\sigma^* \approx \sigma^y$ and $\varepsilon^* \approx \varepsilon^y$. Obviously, the original strip is an excellent tough material, and the toughness of irradiated films worsens with increasing the irradiation time. The strip irradiated for 40 h becomes a typically brittle material.

Figure 4 shows four load–elongation curves measured from the four strips laid at the first (A), second (B), third (C), and eighth (D) layers of the stacked strip specimen after irradiated for 40 h. The change in shape of these load–elongation curves and some others between the third and eighth layers (not shown here) indicates a toughness-to-brittleness variation with a decrease in the ordinal number or the distance to the exposed surface. Comparing curve A with curve B, we can see that the shapes of the two load-elongation curves are quite different from each other: Curve A is a typical load–elongation one for brittle materials, while curve B is a typical load–elongation one for tough materials. This indicates that toughness-to-brittleness variation is very sensitive to the change in distance from the exposed surface to a depth smaller than 8.8 μm.

Figure 5 shows the distance dependence of σ^* (a) and ε^* (b) for the stacked strip samples irradiated for 10, 20, and 40 h. Each point in Figure 5 shows the average value of PET strips with the thickness of 4.4 μm. As we did in Figure 2, this feature is shown by the 4.4 μm bar in Figure 5. From the two plots, we can see that σ^* and ε^* drastically increase from the first point (the first layer) to the second point (the second layer), a distance dependence similar to that shown in Figure 2. Figure 6 shows the irradiation time dependence of normalized stress (a) and strain (b) measured from the strips at the first (0–4.4 μm), second (4.4–8.8 μm), third (8.8–13.2 μm), and fourth (13.2–17.6 μm) layers. Figure 6 shows that below the second layer ($x > 8.8$ μm), the effect of irradiation on the mechanical properties of PET is weak in the time interval covered in this experiment.

Relationship between Molecular Weight and Mechanical Properties

In order to indicate that the decrease in the molecular weight of irradiated PET is one of the main origins causing the deterioration of mechanical properties, σ^* and ε^* are plotted against $\bar{M}_n$, respectively, as shown by $\sigma^* \sim \bar{M}_n$ plot in Figure 7(a) and by $\varepsilon^* \sim \bar{M}_n$ plot in Figure 7(b). For the original strip, $\sigma_0^* \approx 265$ MPa and $\varepsilon_0^* \approx 115\%$; and, correspondingly, its $\bar{M}_n = 18200$. In Figure 7, the points with the highest $\bar{M}_n$ show the values of σ_0^* and ε_0^* of the original film. Only their errors

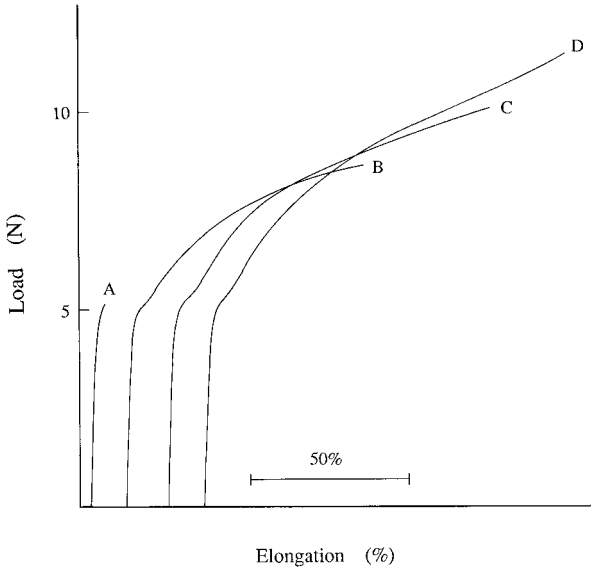

Figure 4 Load–elongation curves of irradiated PET strips located at the first (A), second (B), third (C), and eighth (D) layers after irradiated for 40 h.

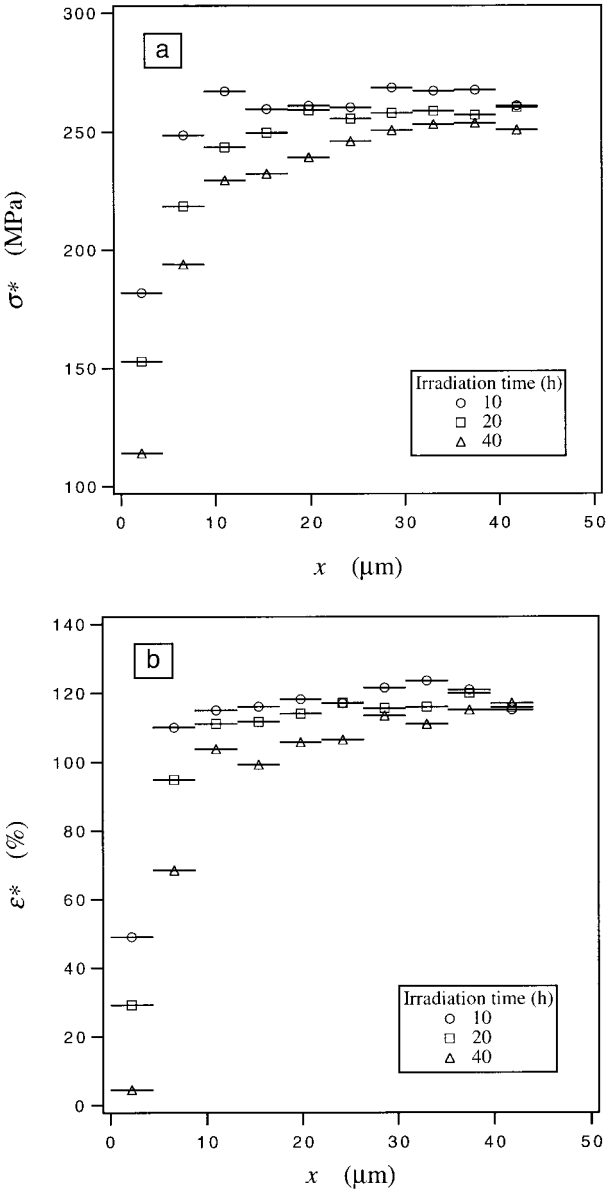

Figure 5 Plots of the stress (a) and strain (b) at break obtained from the irradiated film samples in stack against the distance to the exposed surface x. The irradiation times are indicated in the figure.

are shown in Figure 7 for easily studying the relations between $\sigma^* \sim \bar{M}_n$ and between $\varepsilon^* \sim \bar{M}_n$. Two curves having the shape of the letter S were drawn in the two figures to demonstrate the relations between $\sigma^* \sim \bar{M}_n$ and between $\varepsilon^* \sim \bar{M}_n$. Only the values of σ^* for the strips at the first and second layers irradiated for 50 h are obviously departed from the S-shaped curves. The departure for the strip at the first layer may be because it is difficult to measure correctly the value of σ^* of this very brittle strip. At the movement, we do not know how to explain the departure of the data measured from the strip at the second layer. The data of σ^* and ε^* are scattered at $\bar{M}_n > 14000$, especially for ε^*. However, they are within the error ranges shown in two figures. The errors were induced in preparation of the strips and also during measurement of mechanical properties.

According to the relations between $\sigma^* \sim \bar{M}_n$ and between $\varepsilon^* \sim \bar{M}_n$, we can approximately di-

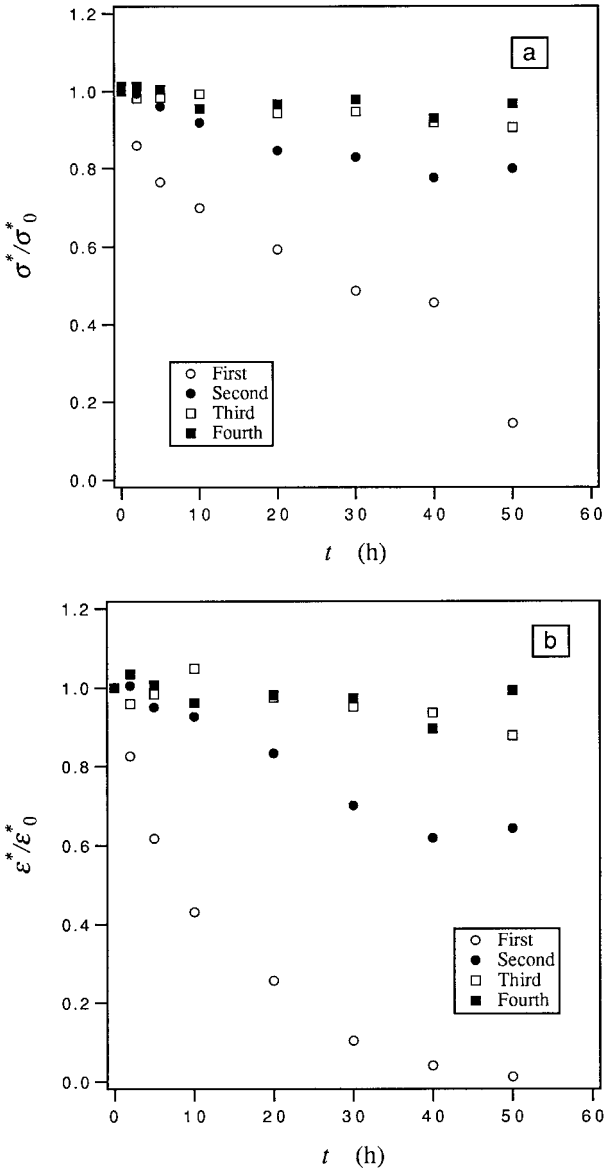

Figure 6 Irradiation time dependence of the normalized stress (a) and strain (b) obtained from the strips at the first (0–4.4 μm), second (4.4–8.8 μm), third (8.8–13.2 μm), and fourth (13.2–17.6 μm) layers of the stacked film samples.

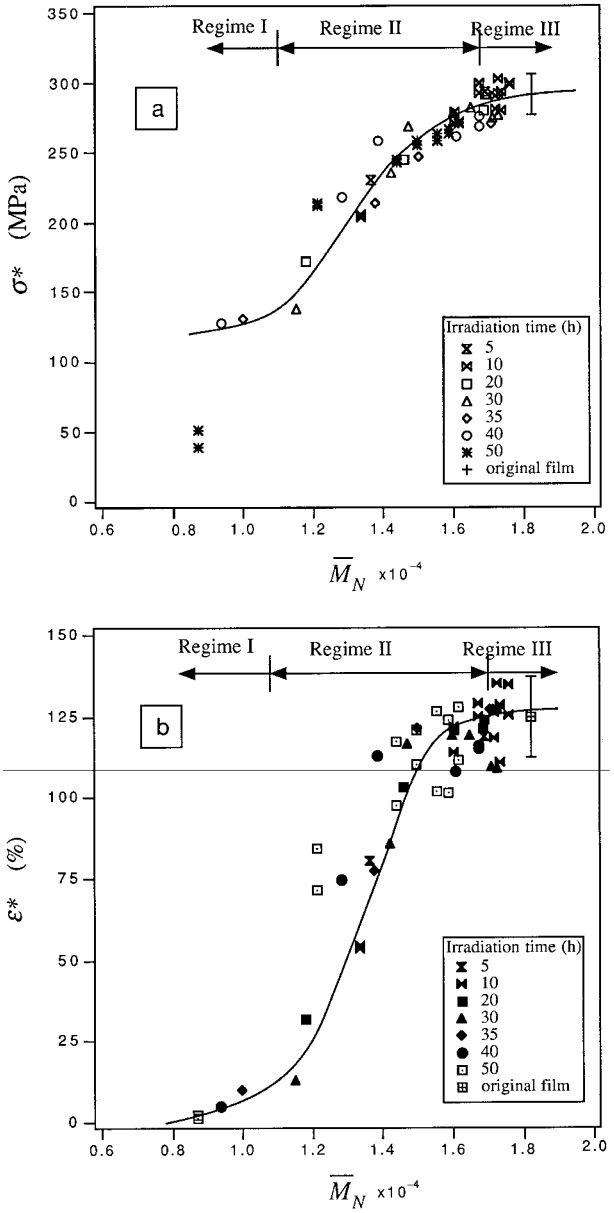

Figure 7 Plots of the stress (a) and strain (b) at break against the number-average molecular weight $\bar{M}_n$. The irradiation times are indicated in the figures.

vide them into three molecular weight regimes I to III, as indicated in Figure 7. In regime I, $\bar{M}_n < 11000$, $\sigma^* \approx \sigma^y$, and $\varepsilon^* < 20\%$ close to ε^y, indicating that the fracture behavior of irradiated strips is similar to that of the brittle materials, as mentioned before. Regime II is in the molecular weight range between $\bar{M}_n \leq 11000$ and $\bar{M}_n \geq 17000$. The most of the measured values of σ^* and ε^* are in regime II. When $\bar{M}_n > 11000$, σ^* and ε^* become to be larger than σ^y and ε^y, indicating that, in this case, the fracture behavior of irradiated strips possesses the feature of tough materials. When $\bar{M}_n$ of irradiated films increases in regime II, the values of their σ^* and ε^* will rapidly approach the values of the original film. When $\bar{M}_n > 17000$, the values of σ^* and ε^* no longer or slowly increase with the increase of $\bar{M}_n$; a plateau regime is reached. Here, we define the regime of $\bar{M}_n > 17000$ as regime III for this PET film.

A–B Model to Describe Fracture Feature of Irradiated Polymers

At first, it is worthy to note that the surface structure of PET observed by transmission electron microscopy has shown no difference before and after irradiation,[18] indicating that UV irradiation cannot directly cause formation of surface cracks. Figures 5(a) and (b) show the relations between the stress and strain at break and the distance to the exposed surface for the stacked film samples after irradiated for 10, 20, and 40 h. The relations may be approximately considered to reflect the changes in the mechanical properties in an irradiated thick PET sample. In this sense, it indicates that the capability to bear a tensile stress for the degraded PET near the exposed surface is much lower than that in bulk. This should be an important origin, which results in a rapid decrease of the mechanical properties of irradiated PET products. In this study a simple A–B model, as shown in Figure 8, is suggested to explain the fracture process and mechanism of irradiated PET samples. The components A and B are composed of the same material but have different mechanical properties, and there is no interface between two. As shown in Figure 8(a), we assumed $\sigma_A^* \gg \sigma_B^*$, $\varepsilon_A^* \gg \varepsilon_B^*$, and $\phi_A \gg \phi_B$. ϕ_A and ϕ_B are the fraction of the components A and B, respectively, and $\phi_A = 1 - \phi_B$.

When subjected to a tensile stress σ_1, there is a corresponding strain ε_1. If $\varepsilon_A^* \gg \varepsilon_1 \geq \varepsilon_B^*$, the component B will break at first [Fig. 8(b)]. Since $\phi_A \gg \phi_B$, the break of the component B leads to formation of some small cracks. When the tensile stress increases to σ_2, a large stress (σ_T) concentrates in the tapered part of the crack, and $\sigma_T > \sigma_A^*$. Thus, the cracks rapidly propagate into the component A since there is no interface between two components [Fig. 8(c)]. At σ_3 and ε_3, which are still smaller than σ_A^* and ε_A^*, the component A breaks [Fig. 8(d)]. Although this A–B model is a parallel one, σ_3 may be smaller than a fracture stress σ_{AB}^* calculated according to the parallel model ($\sigma_{AB}^* = \sigma_A^* \cdot \phi_A + \sigma_B^* \cdot \phi_B$) because the break

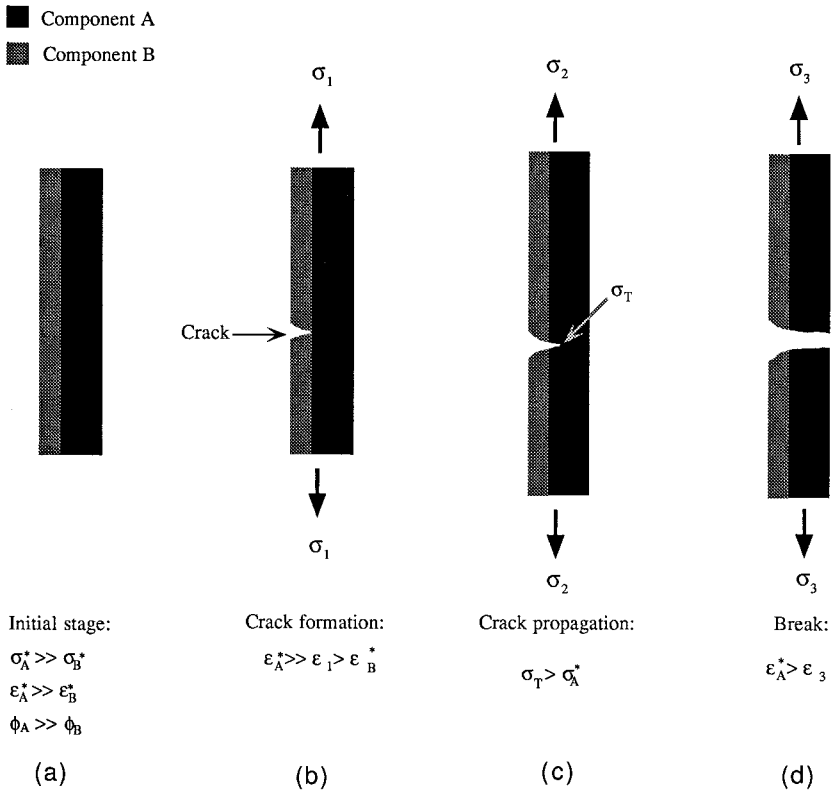

Figure 8 Suggested A–B model to explain the fracture process of irradiated PET and other polymers.

of the component B initiates formation of the cracks; the cracks rapidly propagate into the component A and consequently cause the fracture of the component A.

Rate of Bond Rupture Determined from Stacked Film Samples

Because we have indicated that the decrease in the molecular weight is one of the main origins causing the deterioration in the mechanical properties, in this subsection, we will quantitatively study the photodegradation process developing in a solid PET by studying the photodegradation process of stacked film samples. At first, we shortly discuss the method suitable to analyzing the degradation kinetics based on the experimental data obtained from the stacked film sample. Here, we assume that the decay in the intensity of light irradiation in a polymer along the irradiation direction obeys the Lambert–Beer relation $I = I_0 e^{-\alpha x}$. α is the polymer's absorption coefficient (cm^{-1}), and I_0 the intensity of incident irradiation (photon cm^{-2} s^{-1}). At x depth, there is

$$\frac{N}{\bar{M}_{nt}(x)} = \frac{N}{\bar{M}_{n0}} + \phi_{cs} v I_0 \alpha e^{-\alpha x} t \qquad (2)$$

where t is the irradiation time (s), ϕ_{cs} is the quantum yield of chain scissions per absorbed photon, v is the specific volume (cm^3 g^{-1}) of the polymer, and N is Avogadro's number.[12,13] The molecular weight $\bar{M}_{nt}(x)$ of the irradiated polymer is a function of the distance (x) to the exposed surface of irradiated samples at an irradiation time t. Here, we define the rate of bond rupture $k(x) = \phi_{cs} v I_0 \alpha e^{-\alpha x}/N$, which clearly depends on the distance and has a maximum at $x = 0$ (on the exposed surface).

In this work, the sample composed of stacked films with the same thickness l was irradiated for different times; and, further, $\bar{M}_{nt}$ of each layer was determined. In this case, the average value, $\bar{M}_{nt}(i)$, of the number-average molecular weight for ith layer is

$$\frac{N}{\bar{M}_{nt}(i)} = \frac{N}{\bar{M}_{n0}} + \phi_{cs} v I_0 e^{-\alpha(i-1)l} \frac{1 - e^{-\alpha l}}{l} t \qquad (3)$$

which is obtained by integration[12,13]

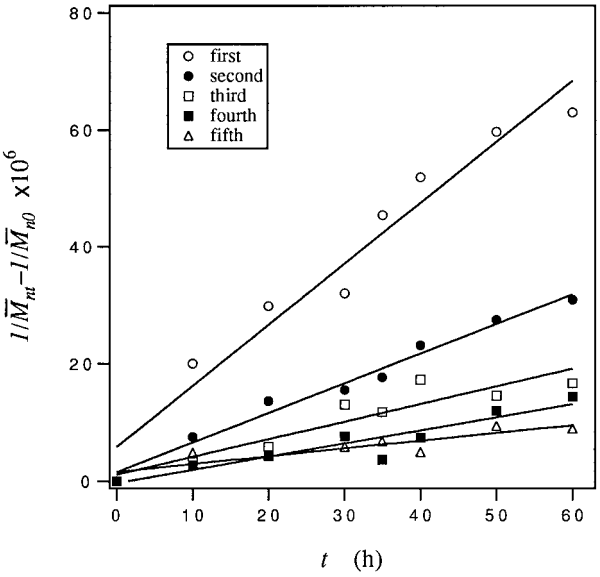

Figure 9 Change in reciprocal number-average molecular weight as a function of irradiation time for the PET films from the first to the fifth layers in the stacked film samples.

$$\frac{N}{\bar{M}_{nt}(i)} = \frac{N}{l}\int_{(i-1)l}^{il}\frac{dx}{\bar{M}_{nt}(x)}. \qquad (4)$$

The average rate of bond rupture for ith layer is

$$\bar{k}(i) = \phi_{cs} v I_0 e^{-\alpha(i-1)l}\frac{1-e^{-\alpha l}}{Nl} \qquad (5)$$

which clearly depends on the thickness l and the position $(i-1)$ of the film at the stacked film samples.

Figure 9 shows a plot of $(1/\bar{M}_{nt}(i) - 1/\bar{M}_{n0}) \sim t$ for the irradiated PET films laid in the first to the fifth layers (i = 1 to 5). The experimental points show scatter to a certain extent but can best be represented by straight lines, which was obtained by the method of least squares. The average rate of bond rupture $\bar{k}(i)$ for each layer, derived from the slopes of the straight lines in Figure 9, are logarithmically plotted against $(i-1)l$ in Figure 10. The slope of the straight line, which was obtained according to the least squares method, in Figure 10 is 0.11 μm^{-1}, corresponding to the absorption coefficient α of PET. Its intercept corresponds to the logarithmic value of the term ϕ_{cs}vI$_0$ $(1-e^{-\alpha l})/Nl$. From them, we obtain the relation of the rate of bond rupture to the distance to the exposed surface, as follows:

$$k(x) = 1.17 \times 10^{-6}\, e^{-0.11x} \qquad (6)$$

with a unit of h^{-1} for the irradiator and the conditions used in this study. Unfortunately, in this work, we cannot determine the quantum yield because it is difficult to determine the intensity of incident irradiation I_0 of this irradiator. It is worthy to note that the relation shown by eq. (6) may be underestimated due to neglecting the light reflection at film–air interfaces.

Figure 11 shows the calculated rate of bond rupture $k(x)$ as a function of x for the PET sample. At the same time, $\bar{k}(i)$ is also plotted against x in the figure when $x = l/2 + l\cdot(i-1)$ and l = 4.4 μm. From an outward perspective, $\bar{k}(i)$ coincides well with $k(x)$. This is because a thin PET film was used in this work and also because of a relatively small value of α = 0.11 μm^{-1}. In these cases, $(1-e^{-\alpha l})/l \approx \alpha$ so that $\bar{k}(i) \approx k(x)$. Figure 11 clearly shows that the largest rate of bond rupture occurs on the exposed surface. Figure 12 shows the calculated molecular weights as a function of x for the PET sample with $\bar{M}_{n0}$ = 18000 at t = 10, 30, and 50 h. Meanwhile, the calculated results (solid lines) are compared with the experimental data (symbols) determined from the stacked film samples in the same conditions when $x = l/2 + l\cdot(i-1)$ and l = 4.4 μm. From Figure 12, we

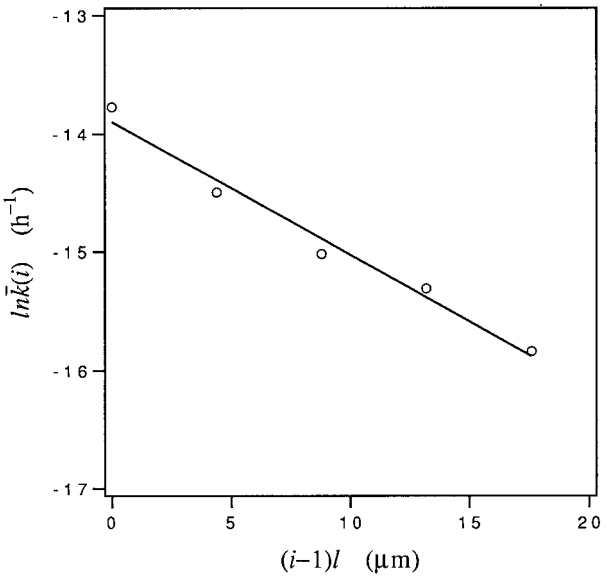

Figure 10 Plot of $\ln\bar{k}(i)$ against $(i-1)l$, as shown with an open circle. The experimental data were fitted according to a linear equation, and a corresponding straight line was drawn in the figure. Its slope is 0.11 μm^{-1}, corresponding to the absorption coefficient of the PET sample.

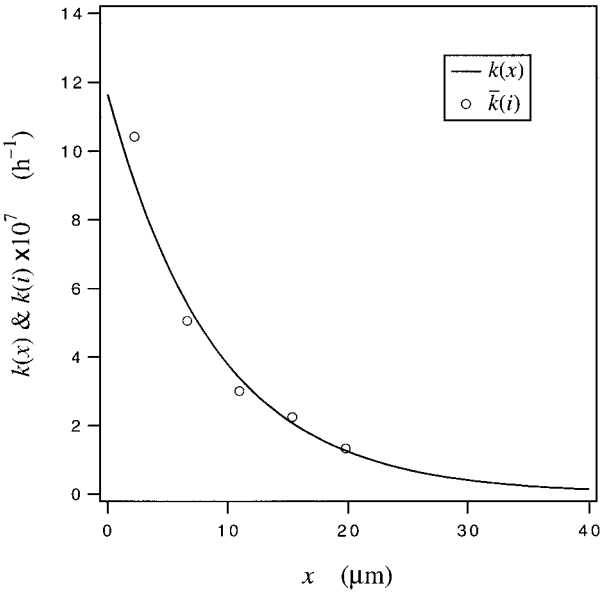

Figure 11 Calculated rate of bond rupture $k(x)$ as a function of the distance to the exposed surface. At the same time, the rate of bond rupture $\bar{k}(i)$ determined from the stacked film samples is also plotted against x in the figure when $x = l/2 + l\cdot(i - 1)$ and $l = 4.4$ μm.

can see that the photodegradation of PET takes place mainly at a layer of about 15 μm in the conditions used in this work.

Before we conclude this article, we want to indicate that if we consider the relationships between σ^* and $\bar{M}_n$ and between ε^* and $\bar{M}_n$ in Figure 7, and, further, if we simply assume that σ^* and ε^* are approximately proportional to $\bar{M}_n$, at least in regime II, we can understand why the distance–dependence of σ^* or ε^* in Figure 5 is similar to the distance–dependence of $\bar{M}_n$ in Figure 2. Correspondingly, the mechanical properties will drastically vary with the distance in the same thickness of about 15 μm, as shown in Figure 5.

CONCLUSIONS

Investigation on the changes in the molecular weight and in the mechanical properties with the distance to the exposed surface for the irradiated stacked PET film samples has elucidated the surface nature of UV deterioration. The relations between the molecular weight and the mechanical properties of the irradiated PET films used were established. The result shows that the decrease in molecular weight is one of the main origins causing the deterioration in the mechanical properties. The photodegradation process developing in PET was quantitatively studied by investigating the degradation kinetics of stacked PET film samples. We obtain the relation between the rate of bond rupture and the distance as $k(x) = 1.17 \times 10^{-6}\, e^{-0.11x}$ (h^{-1}) for the PET sample in the conditions used. It quantitatively demonstrates the surface nature of photodegradation, as follows: The strongest degradation takes place at the exposed surface, and the degradation rate decreases with increasing the distance. Our results further indicate that the degradation of PET macromolecules and the corresponding decrease in the mechanical properties take place mainly in a thin layer of about 15 μm. Therefore, the capability of the degraded thin layer to bear a tensile stress is much lower than that of bulk for irradiated PET. Consequently, irradiated PET may be fractured in a lower stress because the crack can easily form in the thin surface layer when subjected to a tensile stress. The surface nature of the UV photodegradation suggests that to improve the ability of polymers within a thin surface layer to resist UV irradiation is the key factor to protect polymer products. In other words, the UV stabilizers should be primarily distributed in this

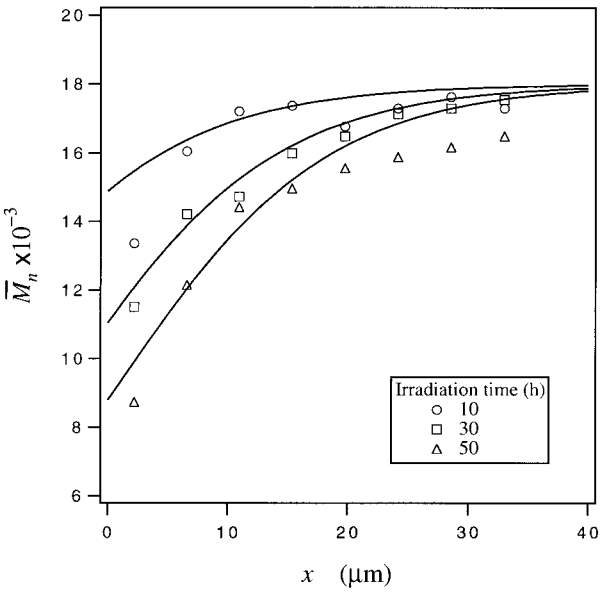

Figure 12 Calculated molecular weights (solid lines) as a function of the distance for PET with $\bar{M}_{n0} = 18000$ at $t = 10$, 30, and 50 h. At the same time, the experimental data (symbols) determined from the stacked film samples in the same conditions are also plotted against x in the figure when $x = l/2 + l\cdot(i - 1)$ and $l = 4.4$ μm.

thin surface layer when they are used for the protection of polymers against UV light.

REFERENCES

1. B. Ranby and J. F. Rabek, *Photodegradation, Photo-Oxidation and Photostabilization of Polymers—Principles and Applications,* John Wiley & Sons, New York, 1975.
2. J. F. Rabek, *Polymer Photodegradation: Mechanisms and Experimental Methods,* Chapman and Hall, London, 1994.
3. W. Schefer, *Textile-Rundschau,* **13,** 336 (1958).
4. C. V. Stephenson, B. C. Moses, and W. S. Wilcox, *J. Polym. Sci.,* **55,** 451 (1961).
5. C. V. Stephenson, B. C. Moses, R. E. Burks Jr., W. C. Coburn, and W. S. Wilcox, *J. Polym. Sci.,* **55,** 465 (1961).
6. M. Day and D. M. Wiles, *J. Appl. Polym. Sci.,* **16,** 175 (1972).
7. M. Day and D. M. Wiles, *J. Appl. Polym. Sci.,* **16,** 191 (1972).
8. H. H. G. Jellinek and W. A. Schlueter, *J. Appl. Polym. Sci.,* **3,** 206 (1960).
9. J. Dhanral and J. E. Guillet, *J. Polym. Sci., Part C,* **23,** 433 (1968).
10. F. Golembe and J. E. Guillet, *Macromolecules,* **5,** 212 (1972).
11. J. B. Lawrence and N. A. Weir, *J. Appl. Polym. Sci.,* **11,** 105 (1973).
12. A. R. Schultz, *J. Chem. Phys.,* **29,** 200 (1958).
13. A. R. Schultz, *J. Appl. Polym. Sci.,* **10,** 353 (1966).
14. K. R. Osborn, *J. Polym. Sci.,* **38,** 357 (1959).
15. A. R. Schultz and S. M. Leahy, *J. Appl. Polym. Sci.,* **5,** 64 (1961).
16. A. R. Schultz, *J. Phys. Chem.,* **65,** 967 (1961).
17. E. Dan and J. E. Guillet, *Macromolecules,* **6,** 230 (1973).
18. P. Blais, M. Day, and D. M. Wiles, *J. Appl. Polym. Sci.,* **17,** 1895 (1973).
19. A. Rivaton, *Polym. Degrad. Stab.,* **41,** 283 (1993).
20. A. Casu and J.-L. Gardette, *Polymer,* **36,** 4005 (1995).
21. I. M. Ward, *Nature,* **180,** 141 (1957).